Inorganic Chemistry

Article

pubs.acs.org/IC

M–M Bond-Stretching Energy Landscapes for $M_2(dimen)_4^{2+}$ (M = Rh, Ir; dimen = 1,8-Diisocyanomenthane) Complexes

Bryan M. Hunter,[†] Randy M. Villahermosa,[‡] Christopher L. Exstrom,[§] Michael G. Hill,*[,‡] Kent R. Mann,*[,§] and Harry B. Gray*[,†]

[†]California Institute of Technology, Pasadena, California 91125, United States

[‡]Occidental College, Los Angeles, California 90041, United States

[§]University of Minnesota, Minneapolis, Minnesota 55455, United States

Supporting Information

ABSTRACT: Isomers of $Ir_2(dimen)_4^{2+}$ (dimen = 1,8-diisocyanomenthane) exhibit different Ir–Ir bond distances in a 2:1 MTHF/EtCN solution (MTHF = 2-methyltetrahydrofuran). Variable-temperature absorption data suggest that the isomer with the shorter Ir–Ir distance is favored at room temperature [K = ~8; $\Delta H°$ = −0.8 kcal/mol; $\Delta S°$ = 1.44 cal mol^{-1} K^{-1}]. We report calculations that shed light on $M_2(dimen)_4^{2+}$ (M = Rh, Ir) structural differences: (1) metal–metal interaction favors short distances; (2) ligand deformational-strain energy favors long distances; (3) out-of-plane (A_{2u}) distortion promotes twisting of the ligand backbone at short metal–metal separations. Calculated potential-energy surfaces reveal a double minimum for $Ir_2(dimen)_4^{2+}$ (~4.1 Å Ir–Ir with 0° twist angle and ~3.6 Å Ir–Ir with ±12° twist angle) but not for the rhodium analogue (~4.5 Å Rh–Rh with no twisting). Because both the ligand strain and A_{2u} distortional energy are virtually identical for the two complexes, the strength of the metal–metal interaction is the determining factor. On the basis of the magnitude of this interaction, we obtain the following results: (1) a single-minimum (along the Ir–Ir coordinate), harmonic potential-energy surface for the triplet electronic excited state of $Ir_2(dimen)_4^{2+}$ ($R_{e,Ir-Ir}$ = 2.87 Å; F_{Ir-Ir} = 0.99 mdyn $Å^{-1}$); (2) a single-minimum, anharmonic surface for the ground state of $Rh_2(dimen)_4^{2+}$ ($R_{e,Rh-Rh}$ = 3.23 Å; F_{Rh-Rh} = 0.09 mdyn $Å^{-1}$); (3) a double-minimum (along the Ir–Ir coordinate) surface for the ground state of $Ir_2(dimen)_4^{2+}$ ($R_{e,Ir-Ir}$ = 3.23 Å; F_{Ir-Ir} = 0.16 mdyn $Å^{-1}$).

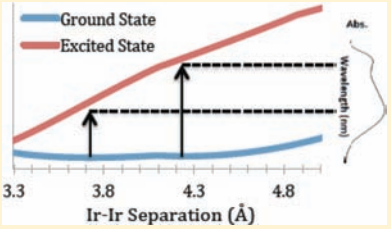

INTRODUCTION

Binuclear complexes of square-planar Rh^I, Ir^I, and Pt^{II} centers have been extensively investigated, owing, in part, to their spectroscopic, photophysical, and photochemical properties.[1−7] The electronic structures of these d^8–d^8 complexes feature a d_{z^2}-derived highest occupied molecular orbital (HOMO) that is σ-antibonding and a p_z-derived lowest unoccupied molecular orbital (LUMO) that is σ-bonding (Figure 1),[8] giving rise to a broad $d\sigma^* \rightarrow p\sigma$ absorption whose position in the spectrum depends strongly on the metal–metal separation.[9−11]

It has been known since 1975 that the rhodium(I) tetrakis(phenylisocyanide) cation dimerizes in concentrated solutions through the formation of an unsupported Rh–Rh bond.[8] In accordance with a d^8–d^8 molecular orbital model,[8] as well as a recent density functional theory (DFT) analysis,[12] the Rh–Rh bond in $[Rh(CNPh)_4]_2^{2+}$ is relatively weak in the ground state (on the order of ~10 kcal mol^{-1}).[9,12] In contrast, Rh–Rh bonding in the $^{1,3}A_{2u}$ ($d\sigma^* \rightarrow p\sigma$) excited states is much stronger,[13] as confirmed by excited-state Raman and time-resolved X-ray diffraction investigations.[14]

Because the $d\sigma^* \rightarrow p\sigma$ transition normally gives rise to a symmetric band in the visible absorption spectrum of a d^8–d^8 complex, we suggested that the decidedly *asymmetric* system observed for a Rh^I dimer bridged by four dimen (1,8-diisocyanomenthane) ligands (Figure 2) logically must be related to an extended Rh–Rh separation imposed by the relatively rigid cyclohexyl unit:[4] the natural bridging distance of dimen is ~5 Å versus the ~3.3 Å separation[15] observed for $Rh_2(TM4)_4^{2+}$, where TM4 = 2,5-diisocyano-2,5-dimethylhexane, a flexible bridging ligand. For $Rh_2(dimen)_4^{2+}$, then, there is a very shallow, anharmonic ground-state potential-energy profile along the Rh–Rh coordinate: dimen strain dominates an energy landscape that is distorted by weak Rh–Rh attraction, giving rise to an asymmetric $d\sigma^* \rightarrow p\sigma$ absorption system.

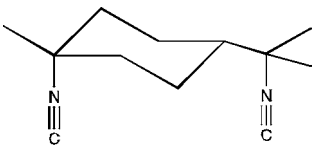

dimen

The spectrum of $Ir_2(dimen)_4^{2+}$ is even richer, showing two distinct absorption maxima (~470 and 580 nm) at room temperature in fluid solutions.[16] On the basis of (1) our serendipitous observation that the color of the Ir^I complex changes reversibly from purple to blue as a function of the

Received: April 6, 2012
Published: May 23, 2012

   dx.doi.org/10.1021/ic300716q | *Inorg. Chem.* 2012, 51, 6898–6905

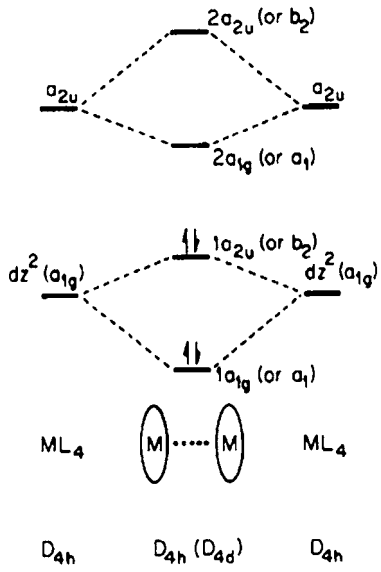

Figure 1. Molecular orbital scheme for d^8–d^8 face-to-face dimers, derived from the a_{1g} (d_{z^2}) and a_{2u} (p_z) monomer functions for $[Rh(CNPh)_4]_2^{2+}$. Reproduced from ref 8.

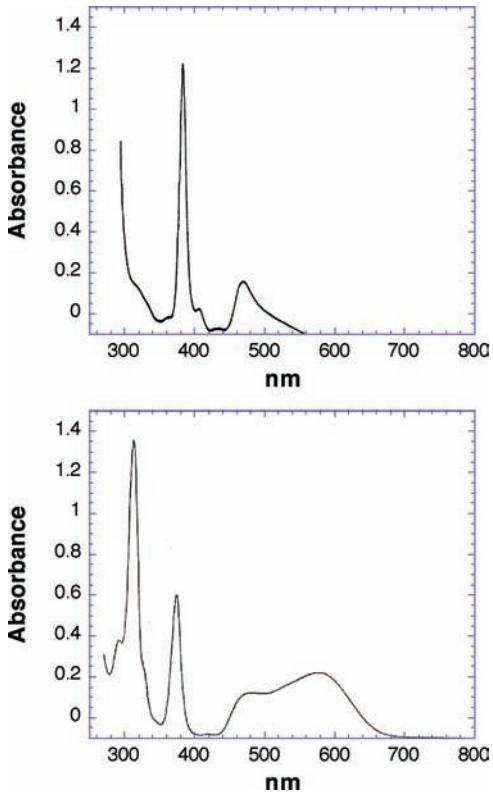

Figure 2. UV–vis absorption spectra: $Rh_2(dimen)_4^{2+}$ (top) and $Ir_2(dimen)_4^{2+}$ (bottom) in a CH_3CN solution.

temperature, (2) the strong correlation between the solid-state Ir–Ir distance and the position of the $d\sigma^* \rightarrow p\sigma$ absorption band for $Ir_2(dimen)_4^{2+}$ salts containing different counterions,[16] and (3) solution Raman data that revealed resonance enhancement of two different Ir–Ir stretching frequencies (12 and 48 cm^{-1}) upon respective excitation into the high- versus low-energy regions of the absorption system,[17] we suggested that $Ir_2(dimen)_4^{2+}$ exists as an equilibrium mixture of two isomers with different Ir–Ir separations in room-temperature solutions. Very recently, this model was supported by independent investigations, one involving ultrafast laser spectroscopy by Gaffney and co-workers[18] and another based on time-resolved X-ray scattering by Haldrup et al.[19] Thus, $Ir_2(dimen)_4^{2+}$ is a rare example of "deformational" isomerism.[20−24]

Noting the head-to-tail asymmetry of the dimen ligand, Haldrup and co-workers suggested that the two Ir–Ir distances of $Ir_2(dimen)_4^{2+}$ arise from different geometric isomers that result from various head-to-tail arrangements of the ligands.[19] Although we cannot rule out this proposal, we favor an alternative explanation here supported by calculations in which the structural elements of $M_2(dimen)_4^{2+}$ have been factored into separate metal- and ligand-based distortions. Overlaying these individual potentials yields composite potential-energy surfaces for $Rh_2(dimen)_4^{2+}$ and $Ir_2(dimen)_4^{2+}$ that are in accordance with all of the experimental data: the Rh^I surface shows a single minimum along the Rh–Rh coordinate, whereas the Ir^I analogue exhibits distinct minima at two different Ir–Ir spacings. Our calculations indicate that the inherent energy required to distort four dimen ligands along the various deformational coordinates (rather than the specific geometric arrangements of the ligands around the d^8 metal centers) can be offset by d^8–d^8 M–M interactions, with the result that there is either a single or double minimum in the potential profile along the M–M coordinate.

EXPERIMENTAL SECTION

The compounds $[Ir_2(dimen)_4][Y]_2$ [Y = PF_6^-, TFPB (tetrakis[3,5-bis(trifluoromethyl)phenyl]borate), and $B(C_6H_5)_4^-$] were prepared according to previously reported procedures.[25] UV–vis spectra were obtained on a Tracor Northern TN-6500 diode-array apparatus employing a xenon arc lamp as the light source. Samples were prepared in a 2:1 mixture of 2-methyltetrahydrofuran (MTHF) and ethyl cyanide (EtCN), which formed a clear, glassy matrix at low temperatures. Variable-temperature measurements were obtained using an Air Products model APD-E temperature indicator/controller. DFT calculations were carried out using the commercial *Gaussian* software package[26] at the B3LYP/6-311G level.[27]

RESULTS AND DISCUSSION

The crystal structures of $[M_2(dimen)_4][Y]_2$ (M = Rh or Ir; Y = PF_6^-, TFPB, and $B(C_6H_5)_4^-$) salts reveal a remarkable range of M–M spacings (3.6–4.5 Å, depending on the identity of M and Y).[16] Moving along the M–M coordinate, the dimen ligands accommodate distances shorter than ~5 Å via two distinct and sequential deformational modes: first, a bending motion in which the isocyano moieties remain eclipsed but "pinch" together; then, at distances < ~3.9 Å, a twisting motion in which the isocyano groups stagger by dihedral angle θ, thereby distorting the ligand backbone (Figure 3). Two geometric motifs, therefore, emerge for $Ir_2(dimen_4)^{2+}$: an eclipsed "paddle-wheel" conformation (Ir–Ir > ~3.9 Å) and a twisted "propeller" conformation (Ir–Ir < ~3.9 Å).

Notably, the solution absorption spectrum of $Ir_2(dimen)_4^{2+}$ exhibits two maxima that are temperature-dependent (Figure 4). The absorption at 470 nm decreases in intensity as the temperature is lowered, while the 580-nm absorption increases. At temperatures lower than ~120 K, only a single maximum (580 nm) is observed. This process is completely reversible, consistent with rapid equilibration of two isomers, "long" and "short" with respect to Ir–Ir distances, each with its signature absorption. On the basis of the solid-state absorption maxima

dx.doi.org/10.1021/ic300716q | *Inorg. Chem.* 2012, 51, 6898–6905

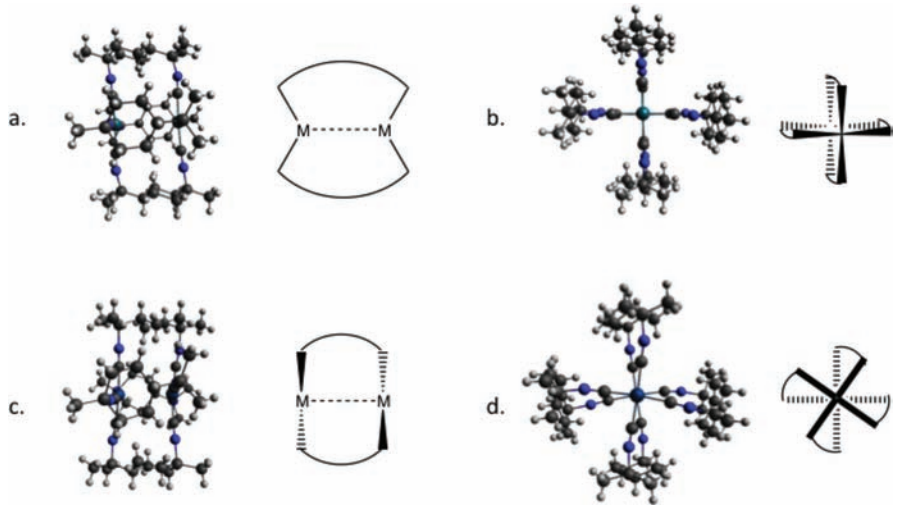

Figure 3. Structural diagrams for the deformational motifs of $Ir_2(dimen)_4^{2+}$: (a) side view of the eclipsed geometry; (b) end view of the eclipsed geometry; (c) side view of the twisted geometry; (d) end view of the twisted geometry.

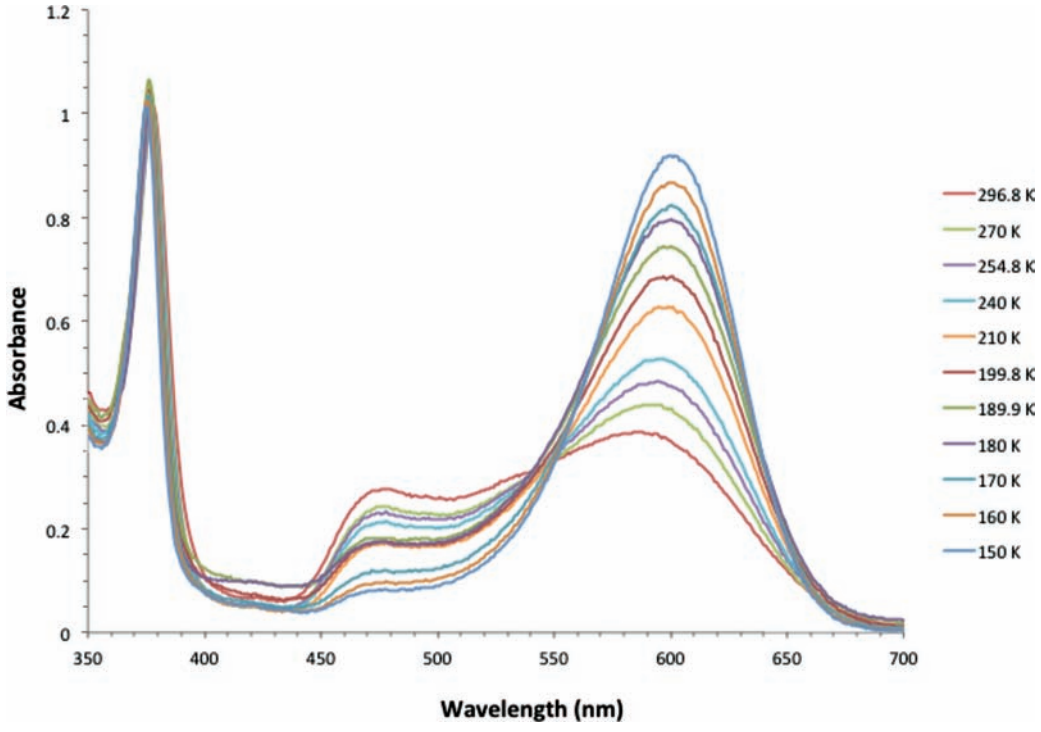

Figure 4. UV−vis absorption spectra of $Ir_2(dimen)_4^{2+}$ in 2:1 MTHF/EtCN recorded between 296.8 and 150 K. Spectra have been corrected for changes in the solvent density and index of refraction.

of the PF_6^- and $B(C_6H_5)_4^-$ salts (λ_{max} = 468 and 580 nm, respectively), we assign the 470-nm band to a paddle-wheel structure that resembles the PF_6^- salt ("long" Ir−Ir distance and eclipsed dimen ligands) and the 580-nm band to a propeller structure resembling the $B(C_6H_5)_4^-$ salt ("short" Ir−Ir distance and twisted dimen ligands). Analysis of these data (see the Supporting Information) yields values of $\Delta H°$ and $\Delta S°$ of −0.8 kcal mol^{-1} and 1.44 cal mol^{-1} K^{-1} for the long ⇔ short equilibrium. On the basis of X-ray structural data,[16] we estimate that the long isomer has an Ir−Ir separation of ∼4.5 Å (dihedral twist angle of 0°), while the short isomer has an Ir−Ir distance of ∼3.6 Å (twist angle near ∼17°).[28,29]

A vibrational wavepacket analysis by Gaffney et al. based on ultrafast transient-absorption data confirms that there are indeed two ground-state Ir−Ir stretches in an acetonitrile solution.[18] To aid in their analysis, these workers also carried out DFT calculations on $Ir_2(dimen)_4^{2+}$. In their simulations, the $[Ir_2(dimen)_4][PF_6]_2$ X-ray structure was optimized under forced C_{2v} and C_2 symmetries, resulting in geometries qualitatively similar to those seen experimentally: C_{2v}, long Ir−Ir distance, eclipsed ligands; C_2, short Ir−Ir distance, twisted ligands (it is of interest that similar findings were reported by Coppens et al. for a related rhodium complex).[30] Although the computations correctly predicted two optimized geometries, the authors noted that they differed quantitatively from the actual (X-ray) structures.[18]

From a structural point of view, the whole-molecule DFT analysis leaves several important questions unanswered. For

dx.doi.org/10.1021/ic300716q | Inorg. Chem. 2012, 51, 6898−6905

example, why are there distinct flexing versus twisting ligand distortions for the long and short isomers? Perhaps more fundamentally, which factors lead to the energetic balance between the two deformational isomers in the first place? In an attempt to answer these questions, we have examined four separate elements of the overall potential surface: (1) a pure metal−metal stretch; (2) an out-of-square-plane bending mode of A_{2u} symmetry; (3) a ligand flexing motion; (4) a twisting of the square planes about the M−M axis. Although we rely on DFT calculations to estimate the energies involved in distorting the dimen ligands, the other deformational energies can be obtained from spectroscopic data.

Metal−Metal Interaction. We first considered the ground-state d^8−d^8 M−M interaction. Previous resonance Raman studies of the $M_2(TM4)_4^{2+}$ analogues of $M_2(dimen)_4^{2+}$ revealed a ground-state ν(M−M) frequency of 55 cm^{-1} for $Rh_2(TM4)_4^{2+}$ and 53 cm^{-1} for $Ir_2(TM4)_4^{2+}$.[10,13] These values yield respective ν(Rh−Rh) and ν(Ir−Ir) force constants of 0.09 and 0.16 mdyn $Å^{-1}$. As expected, ν(Ir−Ir) is much larger in the $Ir_2(TM4)_4^{2+3}A_{2u}$ state (132 cm^{-1}).[10] TM4 features a flexible alkane bridge that allows the metal centers to adopt their preferred "bond" distances. These distances were calculated using Woodruff's relationship,[29] which gives R_e = 3.23 Å for both Rh^I and Ir^I [the calculated Ir−Ir distance in electronically excited ($^{1,3}A_{2u}$) $Ir_2(dimen)_4^{2+}$ is 2.87 Å]. We previously estimated the Rh−Rh bond strength to be 12 ± 6 kcal mol^{-1},[9] and experience suggests that the $5d^8$−$5d^8$ Ir−Ir bond will be stronger (~25 kcal mol^{-1}).

The Morse potential curves for d^8−d^8 Rh^I and Ir^I are shown in Figure 5. Clearly, this potential favors short M−M distances, and Ir^I has a deeper well than Rh^I.

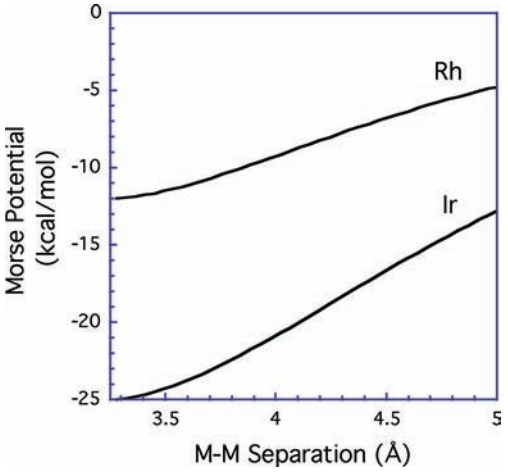

Figure 5. Calculated Morse potentials for the M^I−M^I interaction. Force constants were calculated from experimental Raman frequencies (for Rh and Ir, F = 0.09 and 0.16 mdyn $Å^{-1}$, respectively), and equilibrium bond distances were estimated from Woodruff's relationship (3.23 Å). The Rh^I and Ir^I well depths were estimated to be 12 and 25 kcal mol^{-1}, respectively.

Ligand Strain. Balancing the attraction of the metal centers is the energy required to distort four dimen ligands to accommodate a short M−M separation. Indeed, owing to the relatively weak "bond" between the metal centers, it seemed likely that ligand strain might be the dominant force in determining the optimal M−M separation.

The effect of dimen ligand deformation was explored by performing constrained DFT optimizations on a free ligand. Initially, the isocyano groups were restricted to the same plane. By further constraint of the distance between the two terminal carbon atoms of the isocyano groups (the "bridging C---C" distance), the extent of bending of the ligand was controlled. The C---C parameter was scanned from 3.8 to 4.8 Å, corresponding to a range of 3.2−5.0 Å along the M−M axis (this assumes an average Ir−C bond length of 1.93 Å). Structures were optimized at 0.025 Å increments, and the calculated energy for each structure was multiplied by 4 to account for the entire set of ligands. The relative energies of this "pinching" distortion are plotted versus the corresponding M−M distance in Figure 6 (solid line). The lowest-energy

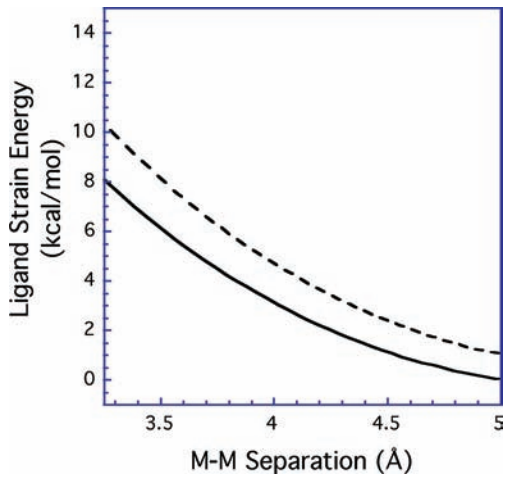

Figure 6. Calculated ligand-strain energy as a function of the M−M separation for $M_2(dimen)_4^{2+}$ complexes constrained such that the square planes are either eclipsed (0° twist angle, solid line) or twisted (10° dihedral angle, dashed line).

conformation of the ligand occurs at an M−M distance of ~5 Å, which is close to that of the experimentally determined "long" form of $Ir_2(dimen)_4^{2+}$. The energy required to distort the ligands to accommodate an M−M distance of 3.5 Å via this pinching mode is ~6 kcal mol^{-1}.

In addition to "pinching", dimen ligands also exhibit a pronounced "twisting" about the M−M axis at shorter M−M distances (<~3.9 Å). Interestingly, this second mode of ligand deformation is not predicted by ligand-based DFT calculations. A second set of optimizations was performed in which the ligand was constrained to a twist angle of 10°, while the M−M coordinate was again scanned. The energy of this "twisting" distortion versus M−M distance (Figure 6, dashed line) shows that the twisted geometry is higher in energy than the corresponding eclipsed geometry *at every metal−metal distance*. Consequently, the ligand-based calculations suggest that the complex should never twist, regardless of the M−M distance.

To address this problem, we examined the localized structural effects of ligand "pinching" versus "twisting" at the metal centers. On the basis of the backbone length of dimen, the individual Ir^I units of an eclipsed (paddle-wheel) dimer can be perfectly planar only at an Ir−Ir spacing of ~4.5 Å. At shorter (or longer) spacings, the dimen ligands pinch (or expand), causing out-of-plane distortions along the A_{2u} bending normal mode at the metal centers. On the other hand, twisting the dimen ligands as the M−M separation becomes shorter

dx.doi.org/10.1021/ic300716q | *Inorg. Chem.* 2012, 51, 6898−6905

allows the ML_4 geometry to retain a *quasi*-planar structure. As such, it is likely that the dimen ligands twist in order to reduce the strain associated with distortion along the A_{2u} bending coordinate.

To quantify this out-of-plane distortional energy, the DFT-optimized structures from the ligand-strain calculations were used to estimate the extent to which each ML_4 center would be deformed under the imposed ligand geometry. The out-of-plane deformational energy was calculated according to

$$E_{A_{2u}} = F\phi^2$$

where F is the force constant given by normal-mode analysis and φ is the magnitude of the distortion from planarity. Because the relevant vibrational frequencies are not known for $Ir_2(dimen)_4^{2+}$, we used the value calculated by Kubas and Jones for the A_{2u} normal mode of $Pt(CN)_4^{2-}$ (0.65 mdyn $Å^{-1}$ rad^{-2}, 93.5 kcal mol^{-1} rad^{-2})[31] as an estimate for F. The rather large force constant for this bending mode presumably originates from disruption of π bonding to CN as the ligands move out of the plane along the A_{2u} coordinate.

Figure 7 shows a plot of this A_{2u} distortional energy as a function of the M−M separation, assuming a perfectly eclipsed

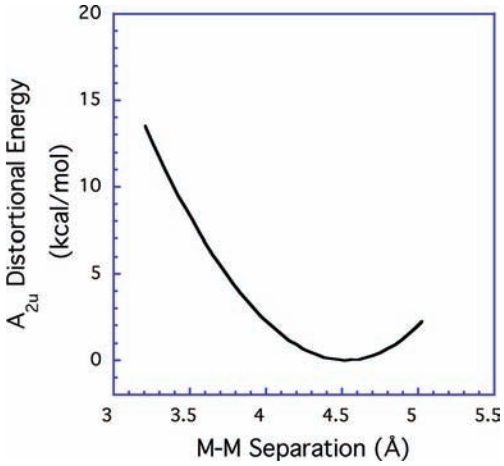

Figure 7. Out-of-plane distortional energy (A_{2u} bending mode with local D_{4h} symmetry) as a function of the M−M distance, calculated for $M_2(dimen)_4^{2+}$ constrained in an eclipsed configuration.

dimen geometry. The magnitude of the A_{2u} out-of-plane bending term is comparable in size to ligand strain, reinforcing the preference for a long M−M distance when the isocyano groups are eclipsed.

Potential-Energy Profiles. The structural elements that determine the preferred M−M separation in $Ir_2(dimen)_4^{2+}$ are (1) an M−M interaction that favors short distances, (2) ligand deformational strain that favors long distances, and (3) an out-of-plane distortional potential that promotes twisting of the dimen backbone at short M−M distances.

Because the ligand-pinching motion is coupled with out-of-plane A_{2u} dynamics, we can revise the Ir−Ir Morse curve to obtain a 2D potential-energy profile for distortion of the eclipsed (0° dihedral, paddle-wheel) structure of $Ir(dimen)_4^{2+}$ along the M−M coordinate. Likewise, we can combine the (higher) deformational-strain energy of the twisted dimen ligands (10° dihedral) with the same Ir−Ir Morse potential to construct the analogous 2D profile that corresponds to the twisted (propeller) form of the complex. These potential profiles are shown along with similarly constructed ones for the paddle-wheel and propeller forms of $Rh_2(dimen)_4^{2+}$ in Figure 8.

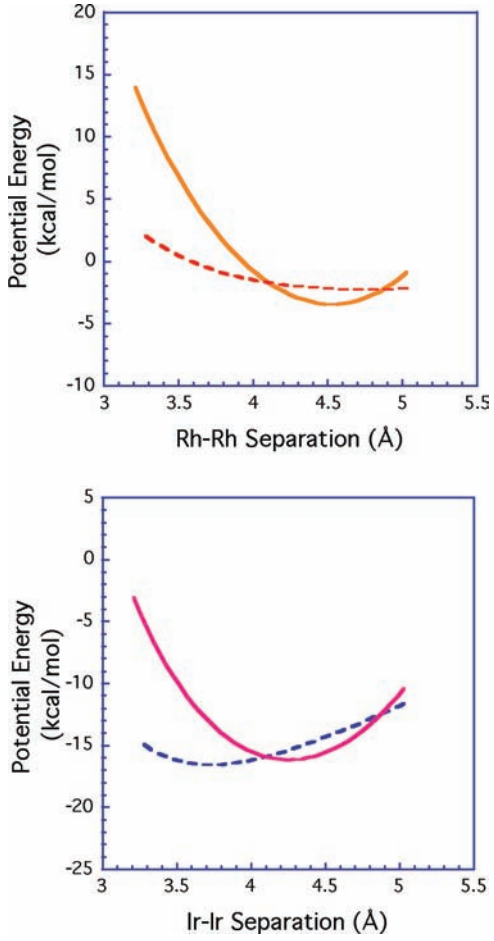

Figure 8. Calculated ground-state potential profiles for $Rh_2(dimen)_4^{2+}$ (top) and $Ir_2(dimen)_4^{2+}$ (bottom). Solid lines indicate eclipsed (0° dihedral angle) ligand conformations, and dashed lines indicate twisted (10° dihedral angle) ligand arrangements. For Ir^I, the eclipsed geometry features a minimum at ∼4.3 Å, while the twisted geometry has a well at ∼3.7 Å. There is a small barrier where the two geometries cross at ∼4.1 Å, which is approximately where twisting occurs in the crystal structures. For Rh^I, the twisted (dashed) potential-energy curve is not sufficiently deep to produce a second minimum at short Rh−Rh distances. Notably, this $Rh_2(dimen)_4^{2+}$ profile is remarkably similar to the surface we predicted[4] based on extensive spectroscopic measurements, and it is nearly identical with the surface calculated by DFT.[35].

Not only do these potential-energy curves reveal the emergence of a double potential-energy minimum for the Ir^I complex, they also explain why the phenomenon is not observed for the Rh^I analogue. At long Ir−Ir distances, ligand geometry and out-of-plane distortional energy dominate the total potential energy, resulting in a "long" isomer with an Ir−Ir distance of ∼4.5 Å, close to the A_{2u} surface minimum. At shorter M−M distances, however, a second region exists in which twisted dimen structures are able to minimize the out-of-plane distortion while maximizing the M−M bonding interaction. These curves cross at an intermediate Ir−Ir separation near 4.1 Å, remarkably close to that observed for $Ir_2(dimen)_4^{2+}$ X-ray structures, which reveal square-plane twisting. In the case of the Rh^I analogue, the Rh−Rh interaction is too weak to produce a second minimum in the short distance

dx.doi.org/10.1021/ic300716q | Inorg. Chem. 2012, 51, 6898−6905

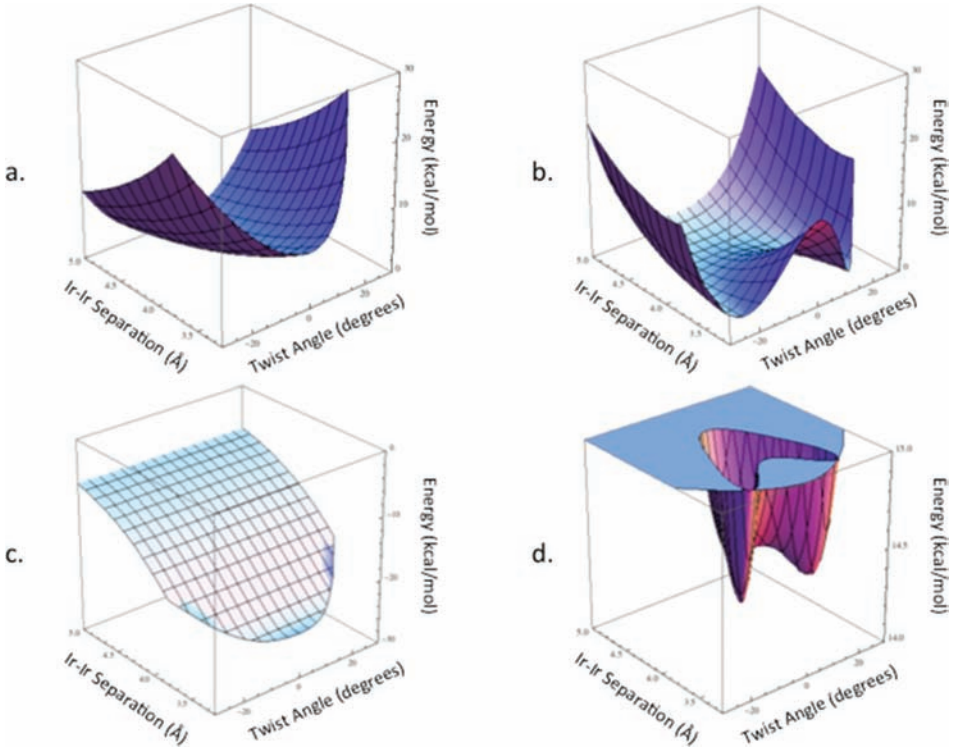

Figure 9. Potential-energy surfaces for $Ir_2(dimen)_4^{2+}$ as a function of the Ir−Ir distance (3.2−5.0 Å) and dihedral twist angle (−30 to +30°): (a) ligand deformation energy; (b) A_{2u} out-of-plane distortional energy; (c) Morse potential; (d) total-energy surface. Vertical axis units are kcal mol^{-1}.

region. Thus, the relatively greater strength of the Ir^I interaction is responsible for the second, low-energy structure, which turns out to be the preferred isomeric form.

3D Potential-Energy Surfaces. 2D slices of far more complicated potential-energy surfaces are shown in Figure 8. Because we wanted to look more closely at transition states, we attempted to calculate a 3D surface for $Ir_2(dimen)_4^{2+}$ as a function of the Ir−Ir separation and ligand dihedral twist angle.

Ligand geometries were independently constrained along both the bending and dihedral twisting coordinates across the range of values found in crystal structures (Ir−Ir 3.2−5.0 Å; dihedral twist 0−30°). These geometries were then optimized, and the deformational energy of four dimen ligands in each of the configurations was plotted as a function of the M−M distance and twist angle (Figure 9a). When symmetry was utilized, positive and negative twist angles were assumed to have the same deformational energy, and the surface was mirrored for −30 to 0°.

Each optimized ligand structure was used to determine the out-of-plane distortion, φ, of an ML_4 center constrained to that geometry. The calculated A_{2u} out-of-plane distortional energy was included in the potential-energy surface shown in Figure 9b. The energetic cost of distorting the metal square planes is substantial, and it is largest for eclipsed ligand structures. We clearly see the benefit of propeller-type geometries; a horseshoe-shaped minimum traces out a set of structures with small out-of-plane distortions that require ligand twisting, thereby demonstrating that this structural element is primarily responsible for the geometrical change from the long to short Ir−Ir form.

The ligand and A_{2u} surfaces were combined with a modified Morse potential for $Ir_2(dimen)_4^{2+}$ (Figure 9c)[32] to produce the potential-energy surface in Figure 9d (a topographical contour map of Figure 9d is given in Figure 10b), which shows three distinct local minima (two are equivalent structures differing only by the twist direction) corresponding to long and short M−M distances. Furthermore, the short form is favored by less than 1 kcal mol^{-1}, and the barrier between the two states is predictably very small. The minima are located approximately at the values expected from the experimental data: ∼4.1 Å/0° twist and ∼3.6 Å/±12° twist.

A contour map of the calculated $Rh_2(dimen)_4^{2+}$ surface is shown in Figure 10a. Because the weaker Rh−Rh interaction is insufficient to overcome the substantial ligand strain and/or A_{2u} deformational energy, the surface features a single minimum at a relatively long Rh−Rh separation (∼4.5 Å) and 0° twist angle. Consistent with our previous spectroscopic analysis, the surface is highly anharmonic.[33]

■ CONCLUSION

In comparing our model to the proposal that head-to-tail ligand arrangements are responsible for conformational isomerism, we emphasize that the explanation offered here is consistent with the temperature dependence of equilibrium $Ir_2(dimen)_4^{2+}$ isomer populations. NMR spectroscopic data show that there is a statistical distribution of ligands at room temperature.[34] Clearly, if the head-to-tail ligand arrangement determines the lowest-energy structure, this distribution would have to change at low temperatures, and it would have to change very rapidly. Ligand substitution on the time scale at which we see equilibration is unlikely.

Our proposed model is also predictive, explaining both the ground-state spectroscopy of $Rh_2(dimen)_4^{2+}$ and the excited-state spectroscopy of $Ir_2(dimen)_4^{2+}$. Electronic absorption data indicate that $Rh_2(dimen)_4^{2+}$ has a single, anharmonic potential-energy surface in the ground state, while $Ir_2(dimen)_4^{2+}$ features minima at two different Ir−Ir distances, a finding that can be attributed to a weaker Rh−Rh interaction. Additionally, because

dx.doi.org/10.1021/ic300716q | Inorg. Chem. 2012, 51, 6898−6905

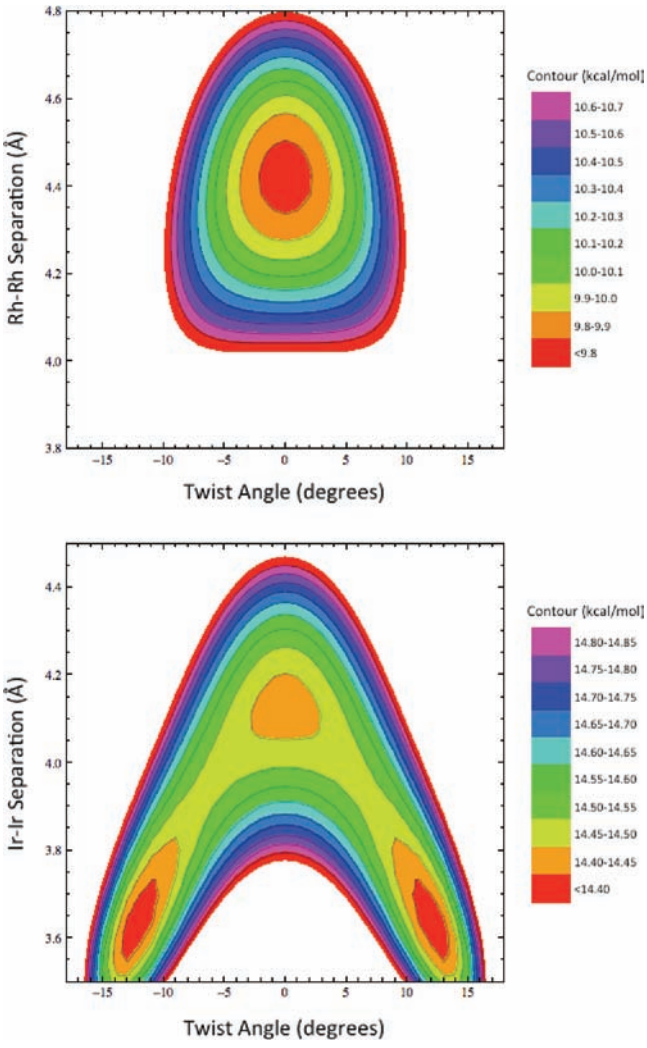

Figure 10. Contour plots of the potential-energy surfaces for $Rh_2(dimen)_4^{2+}$ (top) and $Ir_2(dimen)_4^{2+}$ (bottom).

$M_2(dimen)_4^{2+}$ $d\sigma^* \rightarrow p\sigma$ excitation leads to a formal M−M bond, we expect that the increased M−M interaction in the excited state will dominate the surface, thereby eliminating minima at longer M−M distances. The single, symmetric emission band in each of the Ir^I and Rh^I complexes is fully in line with this interpretation.

■ ASSOCIATED CONTENT

Supporting Information

UV−vis Gaussian curve fit (Figure S1), determination of the thermodynamic parameters (Figure S2), computational details (Figures S3−S7), potential-energy landscape of the $[Ir_2(dimen)_4]^{2+}$ excited state (Figure S8), and calculation data (Table S1). This material is available free of charge via the Internet at http://pubs.acs.org.

■ AUTHOR INFORMATION

Corresponding Author

*E-mail: mgh@oxy.edu (M.G.H.), mann@chem.umn.edu (K.R.M.), hbgray@caltech.edu (H.B.G.).

Notes

The authors declare no competing financial interest.

■ ACKNOWLEDGMENTS

We thank Jay Winkler for helpful discussions. Our work was supported by the NSF Center for Chemical Innovation (Grant CHE-0802907) and by the David & Lucille Packard Foundation Initiative for Interdisciplinary Research. B.M.H. is an NSF Graduate Fellow.

■ REFERENCES

(1) (a) Mann, K. R.; Lewis, N. S.; Miskowski, V. M.; Erwin, D. K.; Hammond, G. S.; Gray, H. B. *J. Am. Chem. Soc.* **1977**, *99*, 5525. (b) Dallinger, R. F.; Miskowski, V. M.; Gray, H. B.; Woodruff, W. H. *J. Am. Chem. Soc.* **1981**, *103*, 1595.

(2) Rodman, G. S.; Daws, C. A.; Mann, K. R. *Inorg. Chem.* **1988**, *27*, 3347.

(3) (a) Smith, D. C.; Gray, H. B. *Coord. Chem. Rev.* **1990**, *100*, 169. (b) Mann, K. R.; Gray, H. B. *Adv. Chem. Ser.* **1979**, *173*, 225. (c) Rice, S. F.; Milder, S. J.; Goldbeck, R. A.; Kliger, D. S.; Gray, H. B. *Coord. Chem. Rev.* **1982**, *42*, 349. (d) Roundhill, D. M.; Gray, H. B.; Che, C.-M. *Acc. Chem. Res.* **1989**, *22*, 55.

(4) Miskowski, V. M.; Rice, S. F.; Gray, H. B.; Dallinger, R. F.; Milder, S. J.; Hill, M. G.; Exstrom, C. L.; Mann, K. R. *Inorg. Chem.* **1994**, *33*, 2799.

(5) Connick, W. B.; Marsh, R. E.; Schaefer, W. P.; Gray, H. B. *Inorg. Chem.* **1997**, *36*, 913.

(6) Leung, S.Y.-L.; Lam, W. H.; Zhu, N.; Yam, V.W.-W. *Organometallics* **2010**, *29*, 5558.

(7) (a) Hill, M. G.; Mann, K. R. *Inorg. Chem.* **1991**, *30*, 1429. (b) Hill, M. G.; Mann, K. R. *Inorg. Chim. Acta* **1994**, *243*, 219.

(8) Mann, K. R.; Gordon, J. G.; Gray, H. B. *J. Am. Chem. Soc.* **1975**, *97*, 3553.

(9) Rice, S. F.; Miskowski, V. M.; Gray, H. B. *Inorg. Chem.* **1988**, *27*, 4704.

(10) Smith, D. C.; Miskowski, V. M.; Mason, W. R.; Gray, H. B. *J. Am. Chem. Soc.* **1990**, *112*, 3759.

(11) Miskowski, V. M.; Rice, S. F.; Gray, H. B.; Milder, S. J. *J. Phys. Chem.* **1993**, *97*, 4277.

(12) Grimme, S.; Djukic, J.-P. *Inorg. Chem.* **2011**, *50*, 2619.

(13) Dallinger, R. F.; Carlson, M. J.; Miskowski, V. M.; Gray, H. B. *Inorg. Chem.* **1998**, *37*, 5011.

(14) Coppens, P.; Gerlits, O.; Vorontsov, I.; Kovarlevsky, A.; Chen, Y.; Graber, T.; Gembicky, M.; Novozhilova, I. *Chem. Commun.* **2004**, *19*, 2144.

(15) Mann, K. R.; Thich, J. A.; Bell, R. A.; Coyle, C. L.; Gray, H. B. *Inorg. Chem.* **1980**, *19*, 2462.

(16) Exstrom, C. L.; Britton, D.; Mann, K. R.; Hill, M. G.; Miskowski, V. M.; Schaefer, W. P.; Gray, H. B. *Inorg. Chem.* **1996**, *35*, 549.

(17) Villahermosa, R.; Miskowski, V. M. Unpublished work.

(18) Hartsock, R. W.; Zhang, W.; Hill, M. G.; Sabat, B.; Gaffney, K. J. *J. Phys. Chem. A* **2011**, *115*, 2920.

(19) Haldrup, K.; Harlang, T.; Christensen, M.; Dohn, A.; Brandt van Driel, T.; Skov Kjaer, K.; Harrit, N.; Vibenholt, J.; Guerin, L.; Wulff, M.; Nielsen, M. M. *Inorg. Chem.* **2011**, *50*, 9329.

(20) Kolle, U.; Kossakowski, J.; Klaff, N.; Wesemann, L.; Englert, U.; Heberich, G. E. *Angew. Chem., Int. Ed. Engl.* **1991**, *30*, 690.

(21) Rohmer, M. M.; Benard, M. *Chem. Soc. Rev.* **2001**, *30*, 340.

(22) Comba, P.; Pandian, S.; Wadepohl, H.; Wiesner, S. *Inorg. Chim. Acta* **2011**, *374*, 422.

(23) Petrov, K. T.; Pinter, B.; Veszpremi, T. *J. Organomet. Chem.* **2012**, *706*, 84.

(24) Franzen, S.; Miskowski, V. M.; Shreve, A. P.; Wallace-Williams, S. E.; Woodruff, W. H.; Ondrias, M. R.; Barr, M. E.; Moore, L.; Boxer, S. G. *Inorg. Chem.* **2001**, *40*, 6375.

(25) (a) Smith, T. P. Ph.D. Dissertation, California Institute of Technology, Pasadena, CA, 1989. (b) Sykes, A. G. Ph.D. Dissertation, University of Minnesota, Minneapolis, MN, 1990. (c) Hill, M. G. Ph.D. Dissertation, University of Minnesota, Minneapolis, MN, 1992.

(26) Frisch, M. J.; et al. *Gaussian 03*,, revision C.02; Gaussian Inc.: Wallingford, CT, 2004.

(27) (a) Becke, A. D. *J. Chem. Phys.* **1993**, *98*, 5648. (b) Lee, C.; Yang, W.; Parr, R. G. *Phys. Rev. B* **1988**, *37*, 785. (c) Stephens, P. J.; Devlin, F. J.; Chabalowski, C. F.; Frisch, M. J. *J. Phys. Chem.* **1994**, *98*, 11623.

(28) We could, in theory, estimate the M−M separation based on the vibrational frequencies measured by resonance Raman or wavepacket analysis (ref 18) and the correlations developed by Woodruff (ref 29); however, these correlations break down for very weak M−M interactions, especially at the limit of the long M−M conformational isomer. For the short M−M isomer, we would predict a 3.25 Å Ir−Ir distance. We expect that the actual value lies somewhere between 3.25 and 3.6 Å.

(29) Miskowski, V. M.; Dallinger, R. F.; Christoph, G. G.; Morris, D. E.; Spies, G. H.; Woodruff, W. H. *Inorg. Chem.* **1987**, *26*, 2127.

(30) Novozhilova, I. V.; Volkov, A. V.; Coppens, P. *Inorg. Chem.* **2004**, *43*, 2299 . For computational reasons, the symmetries in this analysis were lowered from ideal C_4/C_{4v} to C_2/C_{2v}..

(31) Kubas, G. J.; Jones, L. H. *Inorg. Chem.* **1974**, *13*, 2816.

(32) For 3D potential-energy surface calculations, the Ir−Ir interaction was estimated to be 18.5 kcal mol^{-1} and the force constant was 0.65 mdyn $Å^{-1}$ (the latter is approximately 4 times larger than the experimentally determined value). The need to increase the Ir−Ir force constant may be related to an overestimation of the A_{2u} distortional energy for twisted geometries.

(33) The calculated surface for the excited triplet of $Ir_2(dimen)_4^{2+}$ shows a single minimum along the Ir−Ir coordinate (see the Supporting Information, Figure S8) corresponding to an Ir−Ir separation of ∼3 Å and a dihedral twist angle of ±16°.

(34) Sykes, A. G.; Mann, K. R. *Inorg. Chem.* **1990**, *29*, 4449.

(35) Coppens, P.; Benedict, J.; Messerschmidt, M.; Novozhilova, I.; Graber, T.; Chen, Y.-S.; Vorontsov, I.; Scheins, S.; Zheng, S.-L. *Acta Crystallogr., Sect. A* **2010**, *66*, 179.